INTERNATIONAL ATOMIC ENERGY AGENCY
UNITED NATIONS EDUCATIONAL, SCIENTIFIC AND CULTURAL ORGANIZATION
INTERNATIONAL CENTRE FOR THEORETICAL PHYSICS
I.C.T.P., P.O. BOX 586, 34100 TRIESTE, ITALY, CABLE CENTRATOM TRIESTE

SMR/382- 36

WORKSHOP ON SPACE PHYSICS:
"Materials in Micorgravity"
27 February - 17 March 1989

"Metallic Solidification"

S. REX
ACCESS e.V.
Aachen
Federal Republic of Germany

METALLIC SOLIDIFICATION

S. Rex
ACCESS - Aachen Center for Solidification in Space
Intzestr. 5, D-5100 Aachen
West-Germany

1. INTRODUCTION

The first systematic reflections concerning the behaviour of melted materials in space date back to the first manned space flights of the Gemini capsules, in the early 60's. The necessity, and the risk, of carrying out in space such indispensable operations as the welding, or brazing, of metal parts of the capsules, led those in charge of these projects to envisaged possible modifications of the various elementary mechanisms involved in the operations, entailed by this new environment. In the course of the programs it became fully evident that many traditional processes in the Science of Materials were strongly influenced by the various effects of gravity. This had not been clearly demonstrated up till then and, in any case, was practically never discussed in the mathematical description of the physical mechanisms involved.

Thus, only in the second approach the microgravity environment was detected to be an outstanding tool for fundamental experimental investigations, e.g., on the solidification of metals. On earth, solidification is always linked to complex interactions of gravity-independant and gravity-dependant heat and mass transport processes (figure 1). However, the proper determination and controlling of the cooling parameters decide on the microstructure of the solidifying metal which drastically influence the mechanical and other physical properties of the casting or ingot (figure 2). It is well known today that systems undergoing transitions between qualitatively different states can become very sensitive to gravity and offer a chance for microgravity experiments of a fundamental nature. However, interface instability is not only a prob-

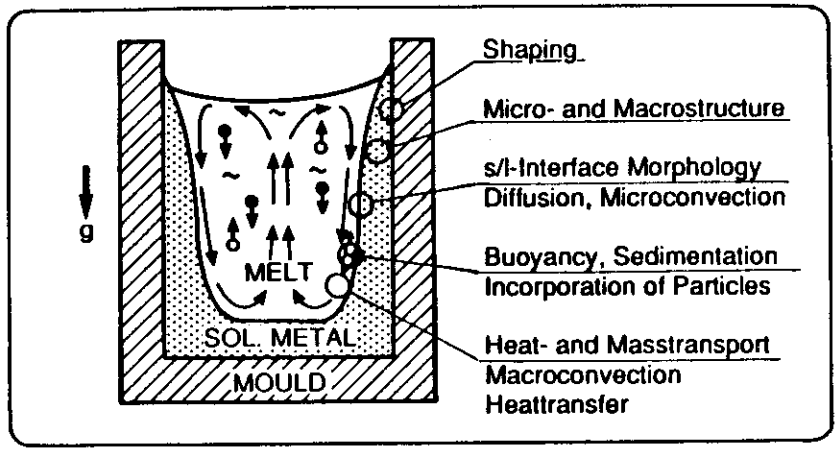

Figure 1: Solidification on earth is linked to a variety dependant and gravity independant processes which determine the formation of microstructure.

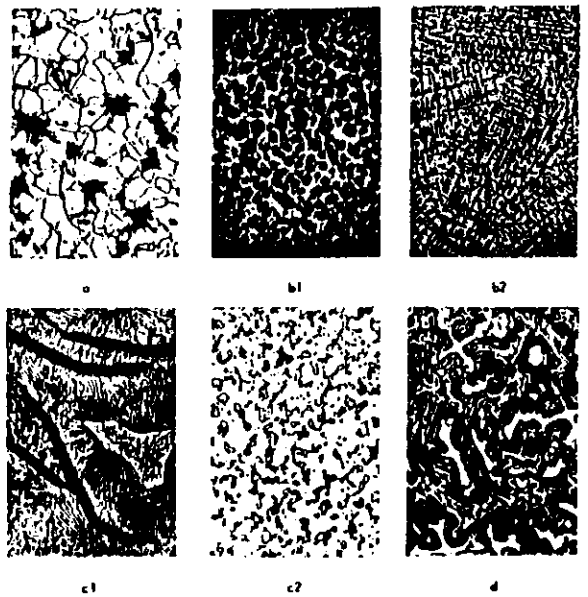

Figure 2: Microstructural elements in one- and more-phase alloys encompass a multitude of phenomena: grain sizes (a) most easily discerned for one-phase alloys such as in the α-, β-, or γ-spaces in a binary A-B system, or grain shapes, for example cells or dendrites (b_1, b_2); eutectic or peritectic phases mostly appear in lamellar shapes or with one phase as fibres (c_1, c_2), the other being the matrix; inclusions normally stem from contaminations, and they assume a host of different shapes, distributions, and locations in the microstructure (d); from Bahm /2/.

lem in itself, but it is also the basic condition to be avoided before performing any crystal growth or solidification experiments.

This lecture which is based for a large part on the textbook of Kurz and Fischer /1/ will lead into the understanding of the basic principles and the mathematical theories of the metallic solidification and finally will give hints to some related objectives for solidification research under microgravity.

2. HEAT EXTRACTION

Without heat extraction there is no solidification. Heat extraction changes the energy of the phases (solid and liquid) in two ways:

a) There is a decrease in the enthalpy of the liquid or solid due to cooling, which is given by:

$$\Delta H = c\, dT \tag{1}$$

b) There is a decrease in enthalpy, due to the transformation from liquid to solid, which is equal to the latent heat of fusion, ΔH_f; defined to be negative for the liquid-to-solid transformation (exothermic reaction).

Heat extraction is achieved by applying a suitable means of cooling to the melt in order to create an external heat flux, q_e. The result cooling rate, dT/dt, can be deduced from a simple heat balance if the metal is isothermal (low cooling rate) and the specific heats of the liquid and the solid are the same. Using the latent heat per unit volume, $\Delta h_f = \Delta H_f/V$, in order to conform with the dimensions of the other factors, then:

$$q_e \left(\frac{A}{V}\right) = -c \left(\frac{dT}{dt}\right) - \Delta h_f \left(\frac{df_s}{dt}\right) \tag{2}$$

c = specific heat per volume; f_s = fraction solid

so that:

$$\dot{T} = \frac{dT}{dt} = -q_e \left(\frac{A}{V}\right) - \left(\frac{df_s}{dt}\right)\left(\frac{\Delta h_f}{c}\right) \tag{3}$$

The first term on the right-hand-side reflects the effect of casting geometry (ration of surface area of the casting, A, to its volume, V) upon the extraction of heat, while the second term to the account to the continuing evaluation of latent heat of fusion during solidification. Heating will occur during solidification if the second term becomes greater than the first one ($\Delta h_f < 0$). This phenomenum is known as recalescence.

For an alloy, where solidification occurs over a range of temperatures, the variation of the fraction solid as a function of time must be calculated from the relationship:

$$\frac{df_s}{dt} = \left(\frac{dT}{dt}\right)\left(\frac{df_s}{dT}\right) \tag{4}$$

since fs is a function of temperature. In this case:

$$T = -q_e \left(\frac{A}{V}\right) \cdot \left(1 + \left(\frac{\Delta h_f}{c}\right) \cdot \left(\frac{df_s}{dT}\right)\right)^{-1} \tag{5}$$

It is seen that solidification decreases the cooling rate since both df_s/dT and Δh_f are negative.

The various solidification processes can generally be distinguished with respect to the way of heat extraction. Figure 3 illustrates two different processes of directional solidification, which means that a thermal gradient is imposed on the sample to achieve a unidirectional (mostly axial) heat flow through the sample. In figure 3a the heat is extracted in an almost steady manner by moving the crucible at a fixed rate through the temperature profile imposed by the furnace. Such a process permits the growth rate of the solid, v (which is not necessarily equal to the rate of crucible movement), and the temperature gradient, G, to be separately controlled. The cooling rate then is related to the other constants by:

$$\dot{T} = G \cdot v$$

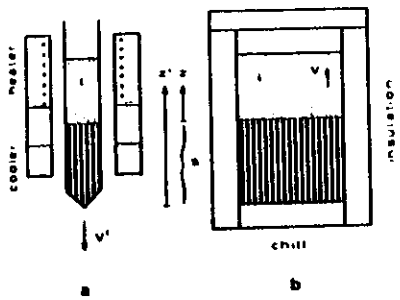

Figure 3: Basic methods of controlled solidification. In directional (Bridgman-type) solidification (a) the crucible is drawn downwards through a constant temperature gradient at a uniform rate, and therefore the microstructure is highly uniform throughout the specimen. The method is restricted to small specimen diameters and, paradoxically, heat must be supplied during solidification in order to maintain the imposed temperature gradient. For these reasons, it is employed only for research purpose and for the growth of single crystals. (b) in directional casting (power-down method) the microstructure is still aligned but no longer uniform along the specimen because the growth rate and the temperature gradient decrease as the distance from the chill block increases.

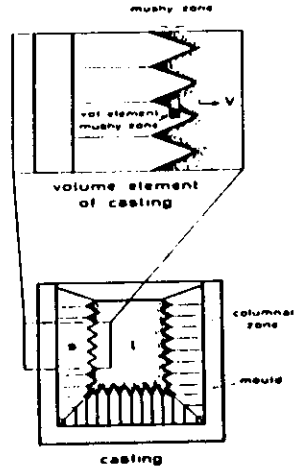

Figure 4: Solidification in conventional castings and ingots. In the vast majority of castings, no directionality is imposed upon the overall structure, but the local situation can be seen to be equivalent to that occuring in directional casting. This is true of the way in which the solid advances inward from the mould wall to form a columnar zone. During the growth of the columnar zone, three regions can be distinguished. These are the liquid, the liquid plus solid (so-called mushy zone), and the solid regions. The mushy zone is the region where all of the microstructural characteristics are determined, e.g. the density, shape, size, and distribution of concentration variations, precipitates, and pores. An infinitesimally narrow volume element which is fixed in the mushy zone and is perpendicular to the overall growth direction permits the description of the microscopic solidification process and therefore of the scale and composition of the microstructure.

In figure 3b the heat is extracted via a chill-block and, as in case 3a, growth occurs in a direction which is parallel, and opposite, to the heat flux direction. In this situation, the heat flux decreases with time as do the coupled parameters, G and v.

Figure 4 shows the solidification in conventional castings and ingots. There is no directionality imposed upon the overall structure, but the local situation can be seen to be equivalent to that occuring in directional casting. Therefore, the results which are obtained in directional solidification experiments can be used to describe the microscopic solidification process in a narrow volume element which is fixed at the solidification interface.

3. MORPHOLOGICAL INSTABILITY OF A SOLID/LIQUID INTERFACE

3.1 Pure Substance

Classical thermodynamic definitions of stability are inapplicable to the determination of the morphology of a growing interface. Therefore, a widely used method in theoretical modelling is the use of stability arguments. These involve perturbing the mathematical function, which describes the solid/liquid interface morphology, in order to determine whether it is likely to change into another one. The interface is said to be morphologically unstable if the perturbation is amplified with the passage of time and to be stable if it is damped out (figure 5).

The conditions which lead to instability can easily be understood in the case of a pure substance. Figure 6 illustrates, in a schematic manner, the development of a perturbation during columnar and equiaxed growth. During columnar growth of a pure substance, the temperature, T_q, increases in the z-direction, i.e. G is positive. The interface will be located at the isotherm where the temperature, T_q, imposed by the heat flux is equal to the equilibrium melting point, T_f. If an interface perturbation is to remain at the melting point over its entire surface the temperature field must be deformed so that the temperature gradient in the solid decreases. Therefore, more heat will flow out of it. As a result, the perturbation tends to be damped out. Thus, the interface of a pure substance during columnar growth will always be stable.

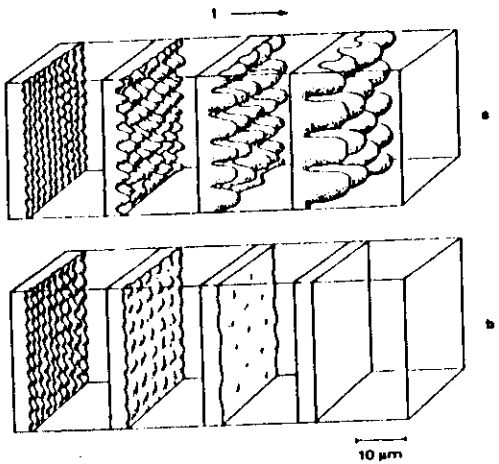

Figure 6: Initial evaluation of an unstable (a) or stable (b) interface. During growth, any interface will be subjected to random disturbances caused by insoluble particles, temperature fluctuations, or grain boundaries. A stable interface is distinguished from an unstable interface by its response to such disturbances. If the distored interface is unstable (a), the projections may find themselves in a more advantageous situation for growth and therefore increase in prominence. In the case of a stable interface (b), the perturbations will be unfavourably situated and tend to disappear.

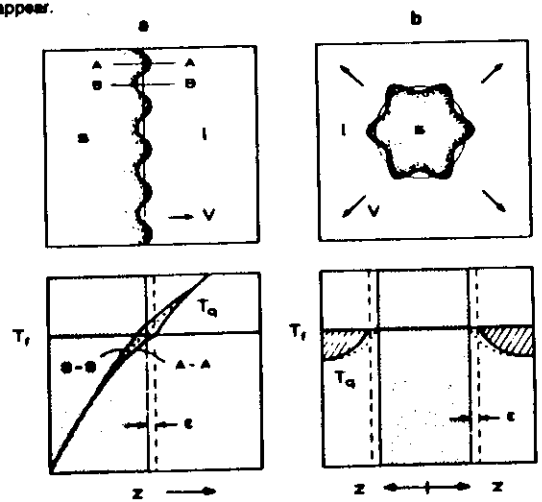

Figure 8: Morphological stability of the solid/liquid interface of a pure substance. In a pure substance, the stability depends only on the direction of heat flow. (a) In directional solidification the heat flux reaches the heat sink via the solid. The temperature always increases with distance ahead of the interface. When a perturbation of amplitude, ε, forms at an initially smooth interface the temperature gradient in the liquid increases while the gradient in the solid decreases. Since the heat flux is proportional to the gradient, the perturbation melts back and the planar interface is stabilized. In equiaxed solidification the opposite situation is found (b). Here, the crystal growth into the undercooled melt (cross-hatched region) and the latent heat also flows down the negative temperature gradient in the liquid. A perturbation which forms on the sphere will make this gradient steeper and, as a result, the local growth rate is increased. The interface is always morphologically unstable.

In the case of equiaxed growth, the situation is completely different. The heat has to be extracted not via the solid but through the melt. Therefore, the melt must be undercooled in order to establish the necessary temperature gradient at the solid/liquid interface. The temperature gradient in the liquid will be negative, while the gradient in the solid is essentially zero. A perturbation will sense a higher gradient at its tip, leading to an increased heat flux, and a resultant increase in the growth rate of the tip. Thus, the interface of a pure substance will always be unstable under equiaxed growth.

3.2 Interface Instability in Alloys

In alloys, the criterion for stable/unstable behaviour is mere complicated because the local equilibrium melting point can vary along the solid/liquid interface. During the solidification of an alloy, solute will pile up ahead of the interface due to the smaller solubility of the solid ($k < 1$). The excess solute rejected from the solid will accumulate in an enriched boundary layer ahead of the interface (figure 7). In the steady-state situation the solid forms at the solidus temperature. Therefore, the composition of the solid is equal to that, c_0, of the liquid far ahead of the interface. The solute concentration in the boundary layer decreases exponentially, from c_0/k to c_0, according to:

$$c_l = c_0 + \Delta c_0 \exp\left[-\frac{v_z}{D}\right] \tag{7}$$

with

$$\Delta c_0 = c_0/k - c_0 = \frac{c_0\,(1-k)}{k} \tag{8}$$

Mathematically, the thickness, δ_c, of the boundary layer is infinite. However, for practical purposes it can be taken to be equal to the 'equivalent boundary layer':

$$\delta_c = \frac{2D}{v} \tag{9}$$

The boundary layer thickness is inversely proportional to the growth rate. The concentration gradient at the interface is given by:

$$G_c = \left(\frac{dc_l}{dz}\right)_{z=0} = -\left(\frac{v}{D}\right)\Delta c_0 \qquad (10)$$

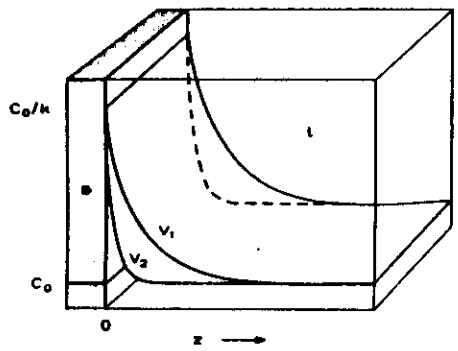

Figure 7: Steady-state boundary layer at a planar solid/liquid interface. As the interface advances, solute is rejected if the solubility of the solid is lower than that of the liquid ($k < 1$). In the steady-state the concentration distribution becomes time-independant. Then the solid concentration is the same as that of the original melt. The concentration in the liquid decreases exponentially from the maximum composition, c_0/k, at the interface to the composition c_0. In general, the rate of rejection of solute is proportional to the growth rate. The rejected solute must be carried away by diffusion down the concentration gradient, and this therefore becomes steeper with increasing growth rate. In the figure, the boundary layers for two growth rates $v_2 > v_1$ are shown.

The concentration boundary layer in front of the solid/liquid interface affects the local equilibrium solidification temperature , T_l, of the liquid, which is related to the composition by:

$$T_l(c_0) - T_l = m(c_0 - c_l) \qquad (11)$$

where $T_l(c_0)$ is the liquidus temperature corresponding to the initial alloy composition. This relationship indicates that the concentration boundary layer can be converted, using the phase diagram, into a liquidus-temperature boundary layer (figure 8). The liquidus temperature increases with increasing z ($k < 1$). It represents the local equilibrium temperature for the solidification of a corresponding volume element of the melt.

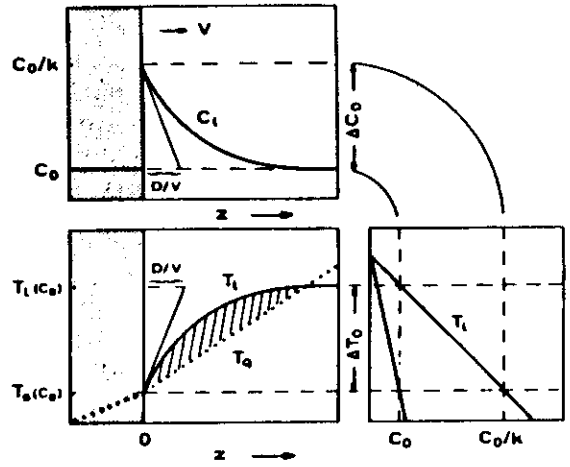

Figure 8: Constitutional undercooling in alloys. The steady-state diffusion boundary layer (figure 7) is shown in the upper diagram for a given growth rate. As the liquid concentration, c_l, decreases with distance, z, the liquidus temperature, T_l, of the alloy will increase as indicated by the phase diagram. This means that the equilibrium freezing points of the liquid vary with position in the manner described by the heavy curve in the lower left diagram. However, the real temperature, T_q, is imposed by the temperature gradient arising from the heat flow. At the solid/liquid interface ($z = 0$), T_q must be equal to T_s. There may exist a volume of liquid which is undercooled when the gradient of T_q is less than the gradient of T_l. This (cross-hatched) region is called the zone of constitutional undercooling. There exists a driving force for the development of perturbation in this volume.

To investigate stability, it is also necessary to consider the temperature, T_q, imposed by the heat flux. Both must be equal at the interface. In the steady-state growth of a planar interface, this will correspond to the solidus temperature for the composition c_0. Depending upon the temperature gradient in the liquid at the interface there may exist a zone of constitutional undercooling (figure 9). The melt in this zone is undercooled, i.e., in a metastable state. It is quickly seen that for the existance of constitutional undercooling the temperature gradient, G, at the interface in the liquid should be lower than the gradient of the liquidus temperature, T_l. The latter gradient is obtained by multiplying the concentration gradient, G_c, by the liquidus slope, m. Therefore, the interface is constitutionally undercooled when:

$$G < m G_c \qquad (12$$

Using equation 10, this can be written:

$$G < -\frac{m v \Delta c_0}{D} = \frac{-m v c_0}{D}\left(\frac{1-k}{k}\right) \qquad (13)$$

Because $-m\Delta c_0 = \Delta T_0$, the limit of constitutional undercooling can be expressed in its usual form:

$$\frac{G}{v} = \frac{\Delta T_0}{D}$$

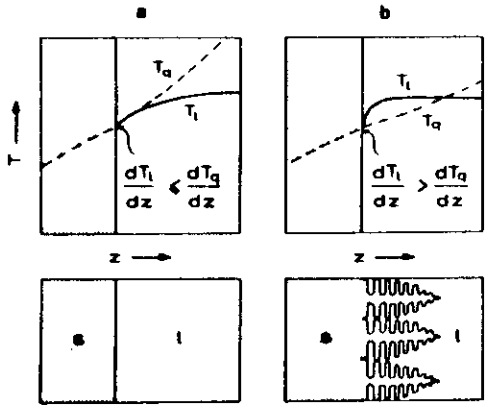

Figure 9: Condition for constitutional undercooling and the resultant structures. When the temperature gradient due to the heat flux is greater than the liquidus temperature gradient at the solid/liquid interface, the latter is stable (a). On the other hand, a driving force for interface change will be present whenever the slope of the local melting point curve at the interface is greater than the slope of the actual temperature distribution. The undercooling encountered by the tip of a perturbation advancing into the melt increases and therefore a planar interface is unstable. After the dendritic microstructure has developed, the region of undercooling is largely eliminated.

4. SOLIDIFICATION MICROSTRUCTURE: CELLS AND DENDRITES

So far, only the limit of stability has been estimated. Nothing has been said about the form and scale of the perturbations which will develop if the interface is unstable. The constitutional undercooling criterion ignores the effect of the surface tension of the interface. A perturbation analysis which takes care of the surface tension and the local interface curvature permits the calculation of the wavelength of the instability which develops. For this purpose it is necessary to suppose that the interface has already been slightly disturbed in a sinusoidal shape. The result is depicted in figure 10 for an Al-Cu alloy and exhibits a characteristic maximum.

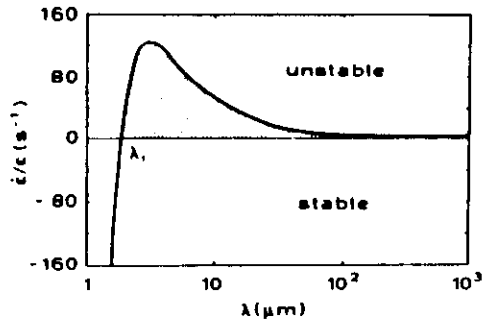

Figure 10: Rate of development of a perturbation at a constitutional undercooled interface (Al-2wt%Cu, v = 0.1 mm/s, G = 10 K/mm). The parameter, $\dot{\varepsilon}/\varepsilon$, describes the relative rate of development of the amplitude of a small sinusoidal perturbation. At very short wavelengths, the value of this parameter is negative due to the curvature damping and the perturbation will tend to disappear. At wavelengths of λ_i and above, the sinusoidal shape will become more accenturated. The wavelength having the highest rate of development is likely to become dominant. The reason for the tendency to stability at high λ-values is the difficulty of diffusional mass transfer over large distance. When the interface is completely stable, the curve will remain below the $\dot{\varepsilon}/\varepsilon = 0$ line for all wavelengths.

Equation 13 in the last chapter focusses attention on the fact that large positive temperature gradients, G_i, provide a stabilizing influence which is less effective when the velocity v increases. The destabilizing influence is provided by the impurity concentration c_0. Figure 11 gives successive steps on the destabilizing process as a function of increasing constitutional undercooling amounts.

In the following we will look at the dendritic solidification in some detail. In figure 12 a single dendrite is depicted schematically which could be thought to be extracted from a dendritic solidification front. Behind the short parabolic tip region perturbations appear on the initially smooth needle as in the case of the breakdown of a planar interface. These perturbations grow and form branches in the four directions which are perpendicular to the trunk. If the primary spacing is sufficiently great, these cell-like secondary branches will develop into dendritic-type branches and lead to the for-

mation of tertiary branches. When the tips of the branches encounter the diffusion field of the branches of the neighbouring dendrite, they will stop growing and begin to ripen and to thicken. Thus, the final secondary spacing will be very different to the initial one. The final value of λ_2 is largely determined by the contact time between the branches and the liquid. This period is known as the local solidification time, t_f, and is given by the time required for a fixed point in the sample to pass from the tip to the root of the growing dendrite.

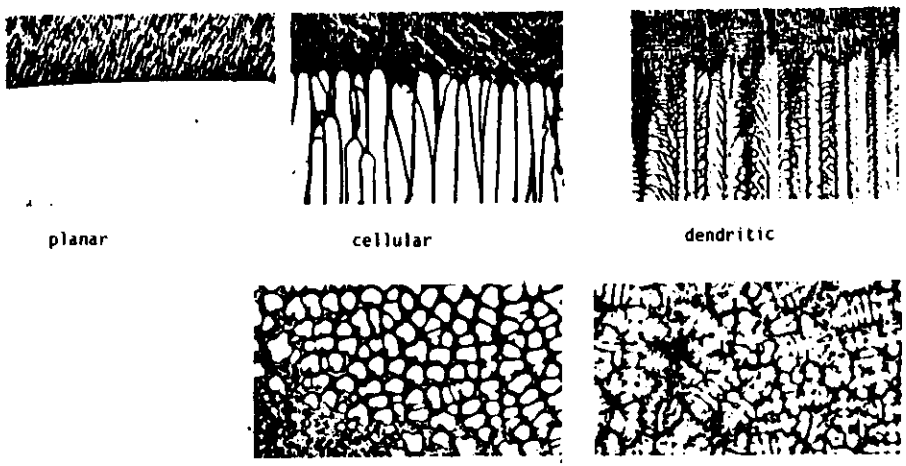

Figure 11: Changing of the morphology of the solid/liquid interface of an Al-0.4wt%Cu alloy with increasing solidification rate at fixed temperature gradients. The quenched interfaces are shown in orientations parallel and perpendicular to the growth direction; from H.M. Tensi /3/.

The growth rate, as well as the dendrite morphology or spacing, are all largely dependant upon the behaviour of the tip region. During the growth of the tip heat and solute are rejected. In the case of directional growth of alloy dendrites the latent heat is transported through the solid, due to the imposed temperature gradient, while solute is rejected ahead of the tips. The rejection of solutes changes the temperature of the solid/liquid interface at the tip. The ratio of the change in concentration of the tip, Δc, to the equilibrium concentration difference, Δc_0, is known as the supersaturation, Ω. This supersaturation represents the driving force for the diffusion of solute at the dendrite tip. The simplest solution for differential equations which describe the solute transport is obtained when the tip morphology is supposed to be hemispherical. The result is that the diffusion boundary layer around the tip is proportional to

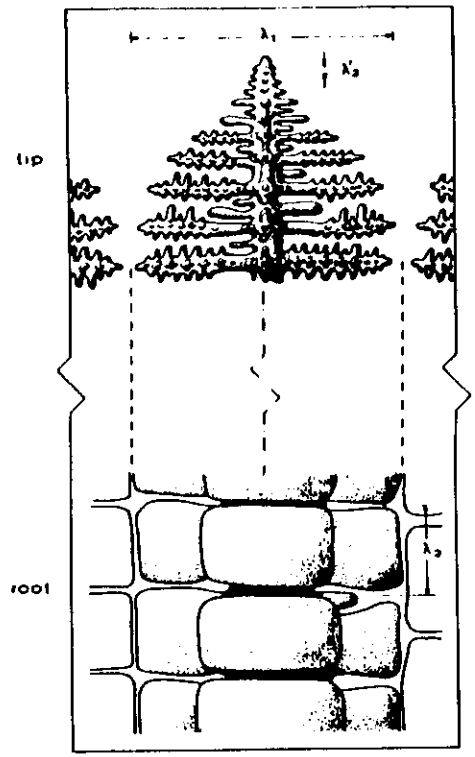

Figure 12: Growing dendrite tip and dendrite root. Depending upon the growth conditions, the dendrite will develop arms of various orders. A dendritic form is usually characterized in terms of the primary (dendrite trunk) spacing, λ_1, and the secondary (dendrite arm) spacing, λ_2. It is important to note that the value of λ_1 measured in the solidified microstructure is the same as that existing during growth, whereas the secondary spacing is enormously increased due to the long contact time between the highly-curved, branched structure and the melt. The ripening process not only modifies the initial wavelength of the secondary perturbations, λ_2', to give the spacing which is finally observed, λ_2, but also often causes dissolution of the tertiary or higher order arms. The two figures are drawn at the same scale, refer to the same dendrite, and illustrate morphologies which exist at the same time but which are widely separated along the trunk length (by about $100\lambda_1$); from Kurz /1/.

the tip radius. Because the gradient of c is inversely proportional to the boundary layer thickness, a sharper tip has a steeper gradient. A sharper tip can grow more rapidly because it can reject solute more efficiently; the flux being proportional to the gradient. However, there is a limit to the possible sharpness of the dendrite tip, R_0, which is represented by the critical radius of nucleation. The overall growth curve of a needle-like crystal, which reflects the sum of the capillarity and diffusion effects, follows the curve in figure 13, and exhibits a maximum close to R_0.

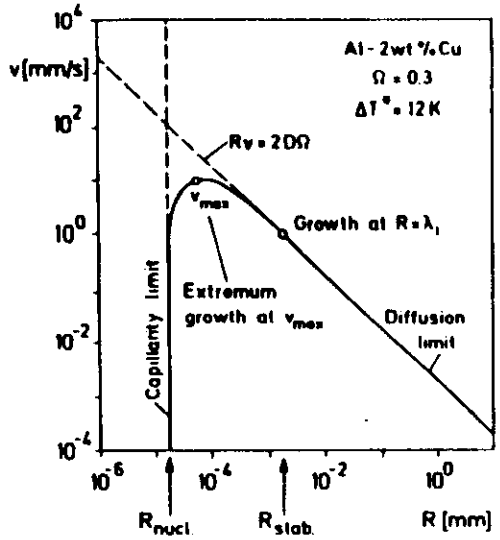

Figure 13: Growth rate of a hemispherical needle. For a given supersaturation, the product, R · v, is constant and means that either a dendrite with a small radius will grow rapidly or one with a large radius will grow slowly. At small R-values, the diffusion limit is cut by the capillarity limit. The minimum radius, R_0, is given by the critical radius of nucleation. Because it was reasoned that the fastest growing dendrites would dominate steady-state growth, it was previously assumed that the radius chosen by the real substance would be the one which gave the highest growth rate, R_m. However, experiments indicate that the radius of the tip is given by the growth condition $R_s = \lambda_i$ when λ_i signifies the onset of the first undulation down the dendrite stem; from Langer and Müller-Krumbhaar /4/.

This maximum was considered to be the radius at which the dendrite would actually grow. Recently, Langer and Müller-Krumbhaar /3/ have argued that a dendrite tip having a small radius tends to increase its radius due to the development of side-branches which interact with the tip. On the other hand, a large tip radius tends to decrease due to the development of instabilities. The result is a growth rate which is associated with a tip having a size at the limit of stability. Thus, the expected tip radius is determined by λ_i, where λ_i is the shortest wavelength perturbation which would cause the dendrite tip to undergo morphological instability. To a first approximation, the wavelength of the favoured perturbation at a planar interface can be used.

Figure 14 shows a plot for the tip radius, R, as a function of growth rate, v, but also a relationship between the primary spacing λ_1, and v, while figure 15 summarizes the main points considered in this chapter. Thus, for one alloy, G and v are the main variables which determine the form and scale of the microstructures.

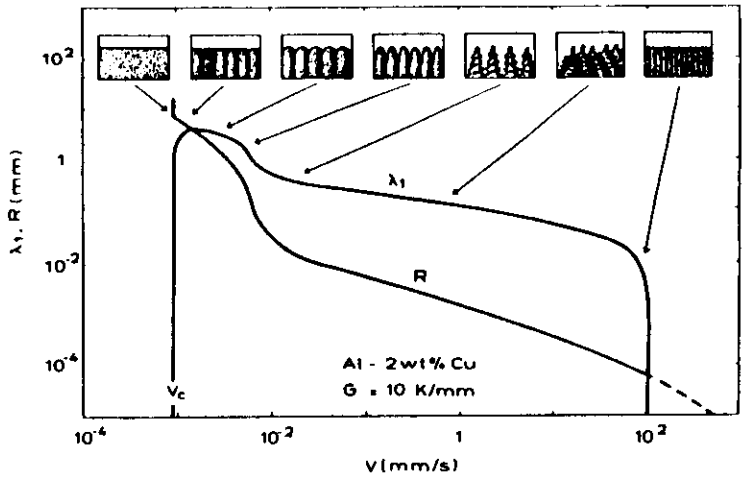

Figure 14: Morphology, tip radius and spacing of cells and dendrites. According to the simple dendrite model, the tip radius decreases from very large values at the limit of constitutional undercooling, v_c, to small values at high growth rates. Over the same range, the primary spacing starts at zero (plane interface), crosses the R-v curve, and reaches zero again at high growth rates. The corresponding interface structures are also shown and vary from planar at growth rates less than v_c to blunt cells, well developed cells and to to dendrites which become finer and finer until they disappear at very high growth rates to give a planar interface again; from Kurz /1/.

5. OBJECTIVES FOR SOLIDIFICATION RESEARCH UNDER MICROGRAVITY

The central purpose of all solidification-linked microgravity research is to increase the understanding of interactions between fluid mechanics and the liquid-solid phase transitions. This may be realized by separating gravity-induced transport mechanisms such as buoyancy, sedimentation, and natural convection from gravity independent processes such as diffusion and specific types of convection in order to study the contributions of single mechanisms to the overall heat and mass transport and to the determination of the growth morphology, table 1.

5.1 Thermo-Solutal Convection

The overall density of a melt is dependant both to its temperature and to its concentration. In the case of vertical directional solidification the positive temperature gra-

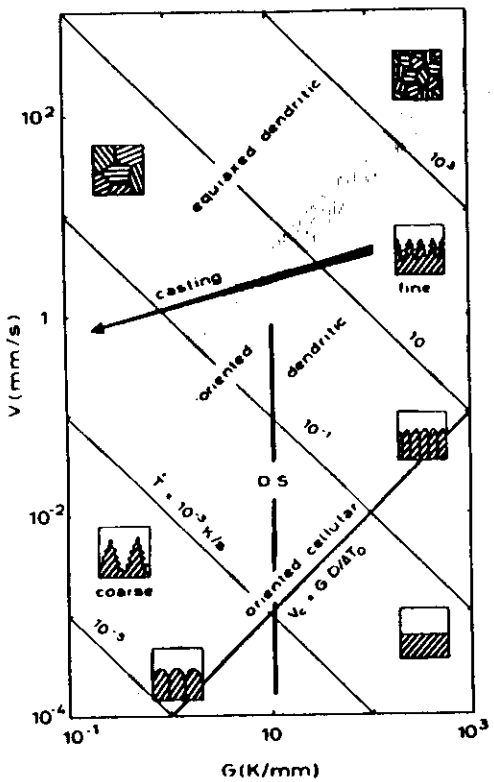

Figure 15: Schematic summary of single-phase solidification morphologies. This diagram summarizes the various microstructures which can be obtained using a typical alloy, with a melting range (ΔT_0) of 50 K, when the imposed temperature gradient, G, or growth rate, v, are varied. Provided that a unidirectional heat flow is imposed, the product, Gv, is equivalent to the cooling rate, $\dot{T}$, which controls the scale of the microstructures formed. The ratio, G/v, largely determines the growth morphology. Moving from the lower left to the upper right along the lines at 45° leads to a refinement of the structure without changing the morphology (G/v = constant). Crossing these lines by passing from the lower right to the upper left leads to changes in morphology (from planar, to cellular, to dendritic growth), and the scale of the microstructure remains essentially the same ($\dot{T}$ = constant). The grey bands define the regions over which one structure changes into another; from Kurz /1/.

dient within the melt stabilizes the density distribution. For all alloys with a solute having the higher density the concentration enrichment in front of the growing interface increases the density, and thus stabilizes the melt as well. In case of less dense solute, however, the overall density profile can become unstable due to the temperature and concentration distribution mix ahead of the interface. This will give rise to the so called thermosolutal convection in the vicinity of the growth front. Due to the strongly different diffusivities of mass and heat transport in metallic melts and also the dependance on melt viscosity the theoretical treatment of the thermosolutal convection is a very complex fluid flow problem. A first approach was delivered by Coriell who numerically calculated a stability diagram for the example of Pb-Sn alloys /5/. With this analysis it was deduced that for low velocities of the interface, the convection instabilities occur at much lower solute concentration than the morphological instabilities, whereas at higher growth velocities the morphological instabilities which are not very dependant of gravity occur at lower concentrations than the convective instabilities (figure 16).

Table 1: Basic microgravity-relevant effects which pervade nearly all of materials processing phenomena (Jansen and Sahm /5/).

GRAVITY-DEPENDANT TRANSPORT PROCESSES:
- Buoyancy and sedimentation induced by $\Delta\rho(T, c)$
- Natural convection induced by $\Delta\rho(T)$ and $\Delta\rho(c)$
GRAVITY-INDEPENDANT TRANSPORT PROCESSES:
- Convection caused by $\Delta\rho$ (liquid/solid-phase transition)
- Marangoni convection induced by $\Delta\sigma(T)$ and $\Delta\sigma(c)$
- Diffusion

5.2 Effect Of Convection On Microstructure

Dendritic growth determines, within a wide region, the microstructure of technical alloys and consequently their properties. Studies dealing with the steady-state growth of a single dendrite have already impressively demonstrated the influence of gravity by using transparent model systems (figure 17). The goal for further investigations consist in understanding also the cooperative growth of arrays of dendrites, i.e. of entire dendritic growth fronts, in order to predict the growth of adjacent dendrites and the associated melt volume. Experiments under microgravity could help to answer such questions about the extend to which convective fluid flow plays a role.

Lately, much attention has been attracted to ripening processes in the mushy zone, i.e. the zone between liquidus and solidus temperature, within dendritic arrays. It is exspected that convection may have an effect on the coarsening behaviour (= ripening) and thus on the final dendrite arm spacing.

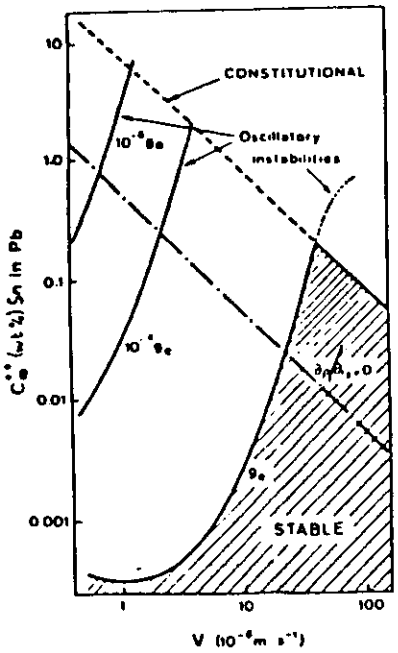

Figure 16: The critical concentration of tin in lead above which instability occurs as a function of growth velocity for a temperature gradient in the liquid, G_l of 200 K/cm. The solid concave curves represent the onset of instabilities of fluid dynamical character for gravitational accelerations g_e, 10^{-4} g_e and 10^{-6} g_e. The upper solid line that slopes downwards to the right represents the onset of constitutionally related morphological instability; Coriell et al. /6/.

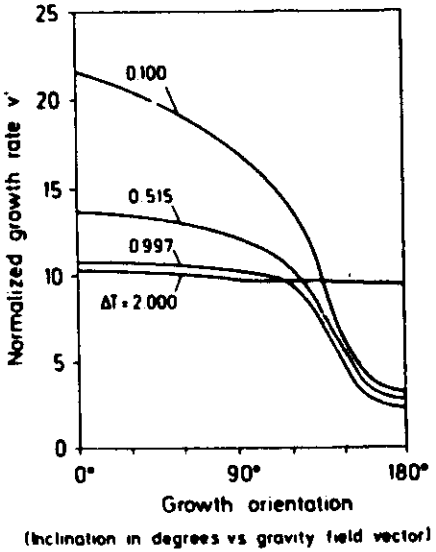

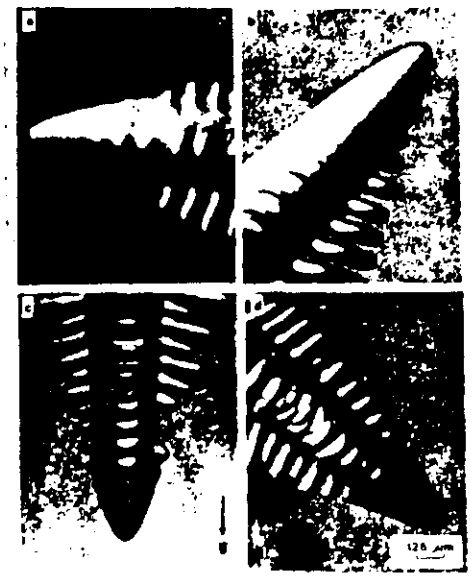

Figure 17: The (normalized) growth rate at low undercooling is sensativaly affected by the gravity vector (a); (b) shows g-vector affected dendrite shape formation; Glicksman and Huang /7/.

REFERENCES

/1/ W. Kurz, D.J. Fischer: "Fundamentals of Solidification". Trans. Tech. Publications (1984)

/2/ P.R. Sahm: In "Convective Transport and Instability Phenomena". Zierep, H. Oertel, G. Braun Verlag, Karlsruhe (1982)

/3/ H.M. Tensi: Maschinenmarkt 83, 7 (1977)

/4/ J.S. Langer, H. Müller-Krumbhaar: Acta Met. 26, 1681-1708 (1978)

/5/ R. Jansen, P.R. Sahm: Mat. Sci. Eng. 65, 199 (1984)

/6/ S.R. Coriell, M.R. Cordes, W.J. Boettinger, R.F. Sekerka: J. Crystal. Growth 49, 13-28 (1980)

/7/ M.E. Glicksman, S.C. Huang: In "Materials Sciences in Space", Conf. Proc., ESA-Report No 142, 309 (1979)